Organic Electronics 13 (2012) 519–524

Contents lists available at SciVerse ScienceDirect

Organic Electronics

journal homepage: www.elsevier.com/locate/orgel

The effect of pH and DNA concentration on organic thin-film transistor biosensors

Hadayat Ullah Khan [a,*,1], Mark E. Roberts [b,2], Olasupo Johnson [b], Wolfgang Knoll [a,3], Zhenan Bao [b,*]

[a] Material Science Group, Max-Planck-Institute for Polymer Research, Ackermannweg-10, D-55128 Mainz, Germany
[b] Department of Chemical Engineering, Stanford University, 381 North South Mall Stanford, CA 94305, USA

ARTICLE INFO

Article history:
Received 12 November 2011
Received in revised form 20 December 2011
Accepted 22 December 2011
Available online 5 January 2012

Keywords:
Organic transistor
OTFT biosensor
pH effects on DNA detection
PNA/DNA hybridization
Titration measurements
Bioelectronics

ABSTRACT

Organic electronics are beginning to attract more interest for biosensor technology as they provide an amenable interface between biology and electronics. Stable biosensor based on electronic detection platform would represent a significant advancement in technology as costs and analysis time would decrease immensely. Organic materials provide a route toward that goal due to their compatibility with electronic applications and biological molecules. In this report, we detail the effects of experimental parameters, such as pH and concentration, toward the selective detection of DNA via surface-bound peptide nucleic acid (PNA) sequences on organic transistor biosensors. The OTFT biosensors are fabricated with thin-films of the organic semiconductor, 5,5′-bis-(7-dodecyl-9H-fluoren-2-yl)-2,2′-bithiophene (DDFTTF), in which they exhibit a stable mobility of 0.2 $cm^2 V^{-1} s^{-1}$ in buffer solutions (phosphate-buffer saline, pH 7.4 or sodium acetate, pH 7). Device performance were optimized to minimize the deleterious effects of pH on gate–bias stress such that the sensitivity toward DNA detection can be improved. In titration experiments, the surface-bound PNA probes were saturated with 50 nM of complementary target DNA, which required a 10-fold increase in concentration of single-base mismatched target DNA to achieve a similar surface saturation. The binding constant of DNA on the surface-bound PNA probes was determined from the concentration-dependent response (titration measurements) of our organic transistor biosensors.

1. Introduction

Improvements in biosensor technology have been realized through an improved understanding of the interface between biology and electronics. While opportunities for electronic detection of biological species using organic transistors are beginning to appear, analysis of biological systems is dominated by more elaborate conventional detection systems. Genetic disease diagnosis and personalized medicine design would benefit tremendously from a low-cost and fast detection tool for DNA hybridization. Hybridization between a dissolved DNA sequence and a surface-tethered complementary DNA (or PNA) sequence is currently evaluated by surface plasmon resonance (SPR) [1,2], surface plasmon fluorescence spectroscopy (SPFS) [3,4], ellipsometry [5] and microgravimetric sensors, including quartz crystal microbalances (QCM) [6] and cantilever based biosensors [7].

Optical measurements provide the bench-mark standard for biological detection applications; however, this method

* Corresponding authors. Tel.: +966 (0)2 808 4519; fax: +966 (0)2 802 1187 (H.U. Khan).
E-mail addresses: hadayat.khan@kaust.edu.sa (H.U. Khan), zbao@stanford.edu (Z. Bao).
[1] Current address: Material Science and Engineering, King Abdullah University of Science and Technology, Thuwal 23955-6900, Saudi Arabia.
[2] Current address: Department of Chemical and Biomolecular Engineering, Clemson University, 204 Earle Hall, Clemson, SC 29631, USA.
[3] Current address: Austrian Institute of Technology, GmbH, Donau-City-Str. 1, 1220 Vienna, Austria.

1566-1199/$ - see front matter © 2011 Elsevier B.V. All rights reserved.
doi:10.1016/j.orgel.2011.12.013

suffers from low throughput and relies on laborious labeling process involving radiolabeled tags or fluorophores and costly detectors [3]. The use of electronic systems for detecting biological species has garnered wide interest due to the simplicity in the detection signal [8,9]. Recent advances in biomolecular detection using OTFTs have shown great promise for a viable and low cost detection systems [10,11]. Despite the wide range of chemical sensing technologies, an inexpensive handheld or easily transportable system for detecting volatile or aqueous analytes with adequate sensitivity, selectivity and reliability still remains elusive. The device stability and biocompatibility for applications aimed at detecting low concentrations of biomolecules in blood or tissue presents significant challenges. Unstable device performance is caused by counterions from the electrolyte migrating into the organic film resulting in leakage current, and redox reactions occurring at the organic semiconductor–electrolyte interface, which irreversibly degrade the organic semiconductor [12].

Two approaches have been described to overcome these issues, which include incorporating thick encapsulation layers of appropriate polymer and using salt-free analyte solutions [13,14]. However, both of these issues directly affect the sensor sensitivity by either blocking the signal or decreasing the Debye screening length [14,15]. Two key challenges facing organic transistor technology must be overcome before these systems can be acceptable for biological detection, which includes: (1) stability of transistor in harsh media (or with variable pH), and (2) selectivity toward a particular analyte with high sensitivity. In our previous work, we improved organic transistor operation stability in water by using low voltage device with robust organic semiconductors [10,16]. We demonstrated the potential application of these transistors as label-free selective DNA sensors [17].

In this report, we characterize the electronic response of OTFT sensor to surface-bound PNA/DNA hybridization in buffer solutions with varying pH, target DNA concentration, and number of base mismatches in the target sequence. Surface titration experiments are used to show the surface saturation as a function of DNA target concentration base mismatches. PNA/DNA titration measurements are characterized by the Langmuir model [18] for the various studied DNA concentrations. The rate constants associated with DNA hybridization are comparable with previously published data [17].

2. Experimental

All materials were purchased from Sigma–Aldrich and used as received unless otherwise stated. The synthesis of the organic semiconductor, 5,5′-bis-(7-dodecyl-9H-fluoren-2-yl)-2,2′-bithiophene (DDFTTF), has previously been reported [10] and is used here as the active organic semiconductor. Thin-films of poly(4-vinylphenol) (PVP) (MW 20,000 g/mol) cross-linked with 4,4′-(hexafluoroisopropylidene) diphthalic anhydride (HDA) were spin-coated according to a previous method [16] and used here as the gate dielectric layer for low-voltage operation. The base sequence of the peptide nucleic acid (PNA) probe (BIO-SYNTHESIS, USA) and target DNA sequences (Eurofins MWG, Germany) are given in Fig. 1a. *N*-ethyl-*N*′-(3-dimethylaminopropyl)-carbodiimide hydrochloride (EDC) and *N*-hydroxysuccinimide (NHS) were purchased from Fluka used to activate the carboxylic acid groups on the sensor surfaces. To prepare phosphate buffer solution (10 mM, pH 7), one phosphate buffered saline tablet was dissolved in 200 mL of deionized water. Eventually one tablet composed of 8.01 g/L NaCl and 0.2 g/L KCl. (calibrated by sigma). Sodium acetate buffer solution (ABS) (stock solution from sigma, 3 M, pH 7) composed of acetic acid and sodium acetate, was diluted in deionized water to achieve 10 mM concentrated solution prior to biosensing experiments.

The fabrication of OTFTs and their use as selective DNA sensors in aqueous media is schematically depicted in Fig. 1b and is given in Supporting information (SI) method [17]. Pulse plasma polymerization of maleic anhydride (ppMA) was used to functionalize the OTFT surface to facilitate the attachment of the PNA molecular probes, more detail can be seen in Supporting information [17]. The density of functional groups, was evaluated using Fourier Transform-Infrared Spectroscopy (FT-IR) (Nicolet 850 Spectrometer) at different input powers, on–off time ratios and depositions times. More detail on FT-IR results described in Supporting information (Fig. S1). Electrical measurements were performed with a Keithley 4200 Semiconductor Characterization System. Electrical sensing measurements were performed under constant bias conditions (V_{DS} = −0.5 V and V_G = −1 V). To ensure a constant analyte concentration, a peristaltic pump (NovoChem) was used at a constant flow rate of 300 μL min^{-1} [17].

3. Results and discussion

Electronic sensors based on OTFTs are evaluated in aqueous media for their performance as selective DNA sensors. Our previously reported aqueous-stable OTFT is used as the sensor platform with a 15 nm film of DDFTTF as the organic semiconductor on a thin polymer dielectric film (20 nm) in PVP–HDA [10,17]. Top-contact OTFTs are fabricated with gold electrodes in a geometry comprising a channel width (W) = 4 mm and length (L) = 50 μm (Fig. 1b). These OTFTs exhibited p-type transistor characteristics at low operating voltages (−1 V) in ambient air and showed an average mobility of 0.45 $cm^2 V^{-1} s^{-1}$ at V_{DS} = −1 V, on/off ratio of 1.5×10^3 and threshold voltage (V_{th}) of 0.045 V (Fig. 2). Moreover, these devices exhibit mobility of 0.2 $cm^2 V^{-1} s^{-1}$ at V_{DS} = −0.5 V in aqueous media (Fig. S2).

PNA/DNA hybridization was carried out between the surface-bound PNA strand and target DNA sequences with varying base mismatches. The designation of the target strands are as follows: fully complementary (**T2-MM0**), one-base mismatch (**T1-MM1**), and two-base mismatch (**T3-MM2**). The use of a PNA probe instead of DNA is an advantageous due to neutral backbone, it can be immobilize on both p-, n-type semiconductor based transistor surface [4,19]. Upon hybridization with the surface-bound PNA, the negative charge in the DNA backbone can therefore influence the current through the p-channel organic semiconductor film during OTFT operation providing a

(a)

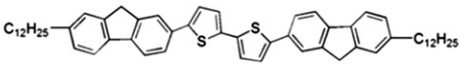

DDFTTF

PNA Probe

P2-15mer 5'-NH_2-OOOOOO TGT ACA TCA CAA CTA-3'

Target DNAs

T2-MM0 3'-ACA TGT AGT GTT GAT-5'

T1-MM1 3'-ACA TGC AGT GTT GAT-5'

T3-MM2 3'-ACA TGC ACT GTT GAT-5'

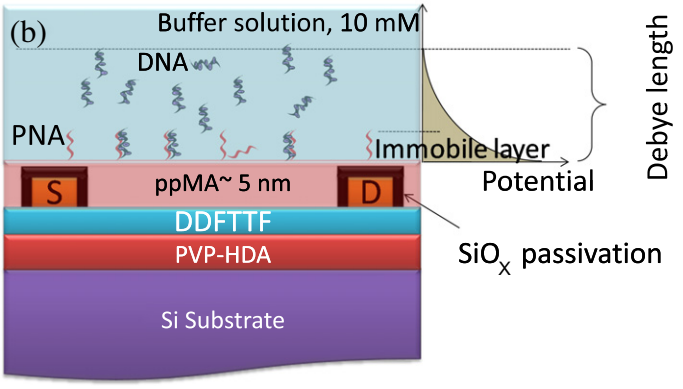

Fig. 1. (a) PNA–DNA 15-mer sequences and the chemical structure of DDFTTF organic semiconductor. Label-free DNA sequences were used for electrical detection with the OTFT sensors. (b) Illustrative schematic of an OTFT DNA sensor. The OTFT consists of a PVP–HDA (20 nm) dielectric layer, DDFTTF organic semiconductor (15 nm), and source–drain (S–D) electrodes with a *W*/*L* of 80. The interdigitated regions of the S–D electrodes were covered with silicon monoxide (thermally-evaporated) and the entire substrate was modified with 5 nm ppMA and PNA probes.

method of sensor response [19]. In an OTFT-based detection system, the occurrence of a chemical or physical absorption (e.g. hybrization of a DNA strand from solution) is converted to a current response (ΔI_{DS}) within the Debye length (λ_D), which ultimately depends on the analyte composition, concentration and pH of the buffer solution [20,21]. Stronger binding, or more efficient hybridization between the DNA and PNA would result in a higher number of negatively-charged DNAs bound to surface, and therefore a larger current change (ΔI_{DS}). The interaction strength can also be determined from the dissociation time [17].

3.1. pH Effect on DNA detection and gate–bias stress

The source of improved sensitivity shown in our previous work was corroborated by conducting the PNA/DNA hybridization diluted in various pH solutions [17]. The influence of gate–bias stress, i.e. the gradual shift observed in baseline-current for constant potential measurements, on the OTFTs was initially evaluated by measuring I_{DS} vs. time for constant source–drain and gate potentials in buffer solutions (10 mM) at either pH 7.4 or pH 7. The baseline-current was recorded for 180 s (Fig. 3a), reveals a less significant change in current at pH 7 compared to pH 7.4 [10].

Further, the influence of gate–bias stress was highlighted by injecting solutions of **T1-MM1** on the OTFT sensor surface with constant and drifting baselines characteristics. **T1-MM1** were used in place of **T2-MM0** due to the weaker hybridization tendency with surface-bound PNA, which allows for partial restoration of the initial baseline-current through rinsing with buffer solution [17]. In this case, multiple association–dissociation sequences could be recorded to examine how these processes vary with time relative to the gate–bias stress effect.

After recording the baseline-current for 60 s, a solution of **T1-MM1** was sequentially injected with intermittent buffer rinses and the change in I_{DS} vs. time was measured. The OTFT current was allowed to equilibrate after each solution exchange. Fig. 3b shows the change in I_{DS} vs. time measurements on a system where the baseline-current was unstable. Reproducible DNA association–dissociation characteristics were obtained when the OTFT response (change in I_{DS} vs. time) to an analyte solution were recorded with improved baseline stability (Fig. 3c). Although the baseline continues to migrate slightly toward a higher current, this dramatic improvement in the sensor evaluation of PNA/DNA hybridization highlights the remarkable sensitivity that can be achieved when the appropriate transistor sensor measurement conditions are implemented.

3.2. Titration experiment and determination of affinity-constant

For DNA detection and mismatch discrimination, we performed titration measurements using three different DNA sequences with equivalent concentrations. Surface

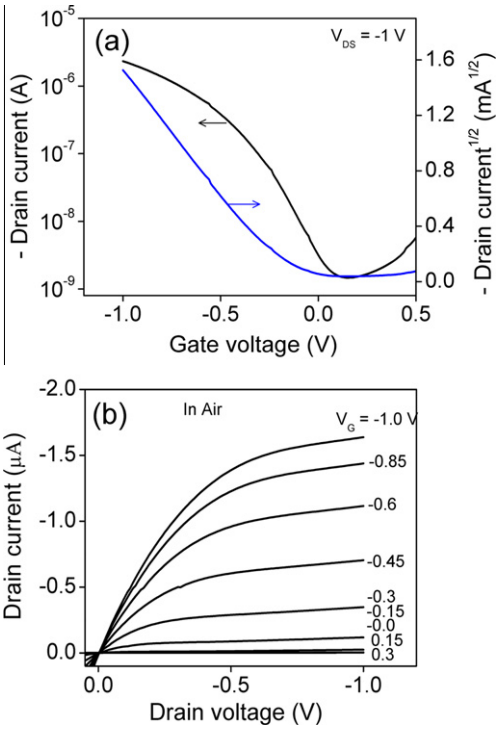

Fig. 2. Electrical characteristics in ambient air with 15 nm DDFTTF on 20 nm PVP–HDA, and source–drain (S–D) electrodes with a W/L of 80. (a) Transfer characteristics (I_{DS} vs. V_G) at V_{DS} of −1 V and (b) output characteristics (I_{DS} vs. V_{DS}) at variable V_G.

titration measurements provide a method for the quantitative evaluation of the hybridization process. According to the Langmuir model, the amount of analyte adsorbed is determined by the equilibrium between free and bound analyte molecules, i.e. the surface coverage (Θ), which corresponds to the maximum change in I_{DS}. This process is repeated with target solutions of higher concentrations until the surface is fully saturated with the target analyte.

The baseline-current was recorded for 100 s, after which a 1 nM solution of **T2-MM0**, diluted in 10 mM buffer solution of pH 7, was injected and the change in I_{DS} was measured with time until the equilibrium was achieved (Fig. 4a). Next, DNA solutions with concentrations of 5, 10, 20, and 50 nM (indicated by arrows in Fig. 4a) were sequentially injected into the flow channel, which resulted in larger changes in I_{DS} owing to higher equilibrium surface coverages. Between sequential target solution additions, a buffer rinsing step was carried out to remove the non-specific DNA from the sensor surface (indicated by thick arrows in Fig. 4a). At equilibrium (i.e. when the current stabilized), the surface was again rinsed with buffer solution. Surface titration with **T1-MM1** was performed in a similar manner and the resulting curve is shown in Fig. 4b. With **T1-MM1**, the equilibrium was achieved at 10-fold higher concentration relative to **T1-MM0**. However, in the titration experiment with **T3-MM2**, the observed signals (change in I_{DS} vs. time) were unstable. Additional titration experiments were performed to validate the titration measurements (Fig. S3).

The changes in drain current (ΔI_{DS}) measured as a function of time during the hybridization reaction can be used to determine the association (k_{on}) and dissociation (k_{off}) rates using Eqs. (1) and (2), based on the Langmuir assumption [4,18]. More detail can be seen in Supporting information:

$$I_{Ci}(t) = (I_{max} - I_o)(1 - \exp(-(k_{on}C_o + K_{off})t)) \quad (1)$$

$$I_{Ci}(t) = (I_{max} - I_o)\exp(-K_{off}t) \quad (2)$$

Fitting each curve in the titration measurement at respective concentration using Eqs. (1) and (2) (red solid curves in Fig. 4a and b), allows for the calculation of the affinity-constants (K_A) = k_{on}/k_{off} i.e. $5.0 \pm 2.6 \times 10^8$ M^{-1} for **T2-MM0** and $1.1 \pm 3.0 \times 10^6$ M^{-1} for **T1-MM1**. The affinity-constant, decreases by two orders of magnitude upon inserting a single base mismatch in the target sequence relative to the complementary sequence, **T2-MM0**. Further support for these data (and for the assumed simple model) comes from the plot of surface coverage (Θ) at specific concentration (C_o) (Fig. 5). A nonlinear steady-state fit using equation $\Theta(C_o) = (K_A \times C_o)/(1 + K_A \times C_o)$ [4,18] allows for the determination of the K_A's, i.e. $4.0 \pm 2 \times 10^8$ M^{-1} for

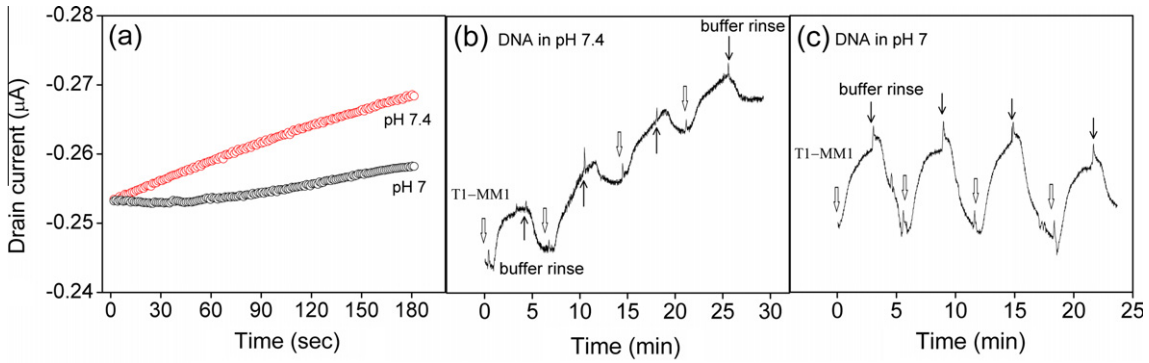

Fig. 3. Baseline and kinetic measurements (current change with time) at constant bias (V_G = −1 V, V_{DS} = −0.5 V) with a solution flow rate of 300 μL min^{-1}. (a) Baseline measurements in buffer solutions with pH of 7 and 7.4. (b) Kinetic sensor measurement on an OTFT with an unstable baseline (modified with PNA probes) targeting the **T1-MM1** DNA sequence. Open down head arrows show the injection of target DNA and solid arrows indicate the switch to buffer solution. (c) Kinetic sensor measurement using an OTFT with improved baseline stability and targeting one-base mismatch DNA (**T1-MM1**).

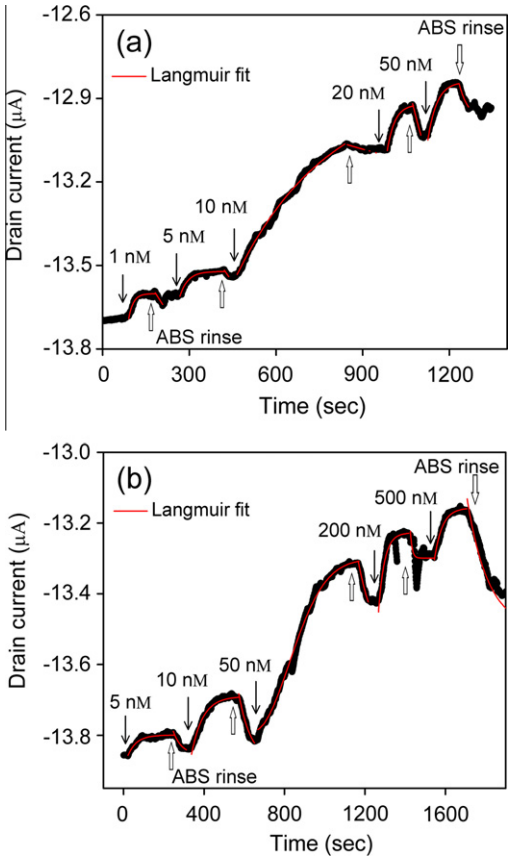

Fig. 4. Titration curves for PNA/DNA hybridization using the DDFTTF OTFT sensor at constant bias ($V_G = -1$ V, $V_{DS} = -0.5$ V) with a flow rate of 300 μL min^{-1}. Solid arrows indicate the additions of target DNA solutions and open arrows indicate the exchange to buffer solutions. The solid red lines show the Langmuir fits. (a) OTFT sensor titration with the **T2-MM0** DNA-15mer and (b) **T1-MM1** DNA-15mer. (For interpretation of the references to color in this figure legend, the reader is referred to the web version of this article.)

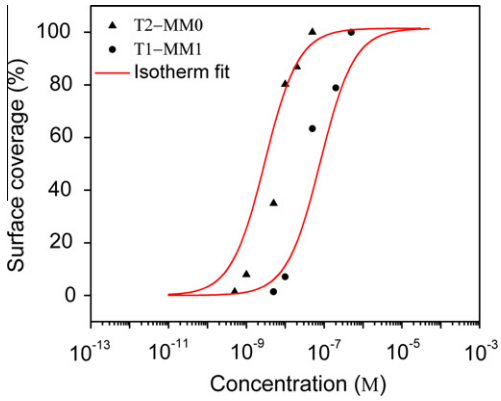

Fig. 5. The Langmuir adsorption isotherm plot between the surface coverage (saturation responses at each concentration) taken from Fig. 4a (**T2-MM0**) and Fig. 4b (**T1-MM1**) vs. target concentration (C_o). The solid S-shaped curves correspond to the fit by the Langmuir isotherm.

T2-MM0 and 0.9 ± 1 × 10^6 M^{-1} for **T1-MM1**, which are consistent to those determined from the average association and dissociation rate constant (Fig. 4a and b).

The decrease in I_{DS} is associated with DNA hybridization and indicates that, in our experiment, DNA is negatively charged at pH 7. The counterions from DNA affect the DDFTTF active layer [17,22] when the negatively charged DNA hybridizes with PNA probe, establishing a longitudinal electrical field streaming potential within λ_D [23]. We assume that this streaming potential is constant because it is a function of flow velocity, which was kept constant 300 μL m^{-1} in all experiments. The λ_D also effects the sensitivity of sensors by competing with the capacitance effect at the surface of the functional layer [24]. Since the λ_D of the 10 mM buffer solution is ~7 nm [15,20], and PNA/DNA hybrid has a thickness of ~2 nm [17], a fraction of the total sensor response, change in I_{DS} signal, will result from the non-hybridized DNA.

Typically in titration experiments, due to variable mismatches in target DNA, high concentration is required to achieve equilibrium. It is well known that the sensitivity is limited by Coulombic repulsion between the nearly saturated surface and DNA from solution. Therefore, additional hybridization was not obtainable without adding a rinsing step between each target concentration addition (Fig. 4a and b). Moreover, we speculate that the Coulombic repulsion limits the detection with two-base mismatched target DNA because as the coverage increases the surface charge density generates an increasingly repulsive Coulombic barrier against further target binding. Operating in high ionic strength buffer solutions or diluting the probe density of the sensor matrix could limit the influence of Coulombic repulsion on the hybridization kinetics [4]; however, both of these conditions would adversely affect the sensor sensitivity. Nonetheless, a control kinetic experiment was performed at higher concentrations where a single injection was used to influence a change in current with each mismatched target DNA sequence (Fig. S4). Although, the signals from the two-base mismatch DNA target revealed a more stable response, the intensity was very weak due to non-specific accumulated DNA [4,25].

4. Conclusion

Label-free electronic biological detection has attracted interest as a means to reduced sample preparation (e.g. target reporter labeling) and detection time and potentially reduce the overall cost and complexity of the analysis systems. In this report, we characterized the affect of DNA hybridization on the electronic response of a PNA-modified OTFTs for sensor applications. A high affinity-constant was extracted from PNA/DNA titration measurements on DDFTTF transistor sensors in the optimized pH solution, which showed excellent discrimination between the complementary DNA target and sequences with single/double base mismatches over a range of concentrations. Surface titration experiments revealed that the equilibrium surface saturation required a 10-fold increase in solution concentration for the single-mismatch DNA target relative to the complementary target. Coulombic repulsion between the

sensor surface and highly concentrated DNA solution became the dominant factor to limit the detection of more than one-base mismatch target. We also showed that the gate-bias stress could be reduced by adjusting the pH toward physiological conditions, which further improved sensitivity for DNA detection. These results indicate that OTFTs are promising for in-situ biosensing.

Author contributions

O.J. designed and fabricates the OTFTs. H.U.K. fabricated and modify the OTFTs using PE-CVD. H.U.K. designed and performed experiments, analyzed data and wrote the manuscript. M.E.R. supervised O.J. to fabricate the OTFTs and contribute mainly for the correction of manuscript. Z.B. directed the OTFTs fabrication and project. W.K. directed all the PNA/DNA sensing measurements and project.

Acknowledgements

H.U.K. acknowledges the financial support from IRTG/1404 (funded by the DFG) and Max Planck Society (Germany). This project was funded by the National Science Foundation Materials Research Science and Engineering Center of Polymer and Macromolecular Assemblies (DMR0 213618), National Science foundation (ECCS0730710) and the Office of Naval Research (N000140810654). M.E.R. acknowledges partial support from the NASA GSRP fellowship; O.J. acknowledges partial support from a Hewlett Packard graduate fellowship. (Supplementary information is available online from Wiley InterScience or from the author).

Appendix A. Supplementary data

Supplementary data associated with this article can be found, in the online version, at doi:10.1016/j.orgel.2011.12.013.

References

[1] A.I.K. Lao, X. Sub, K.M.M. Aung, Biosens. Bioelectron. 24 (2009) 1717.
[2] W. Knoll, Annu. Rev. Phys. Chem. 49 (1998) 569.
[3] T. Neumann, M.-L. Johansson, D. Kambhampati, W. Knoll, Adv. Funct. Mater. 12 (2002) 575.
[4] H. Park, A. Germini, S. Sforza, R. Corradini, R. Marchelli, W. Knoll, Biointerphases 1 (2006) 113.
[5] L. Moiseev, M. SelimUnlu, A.K. Swan, B.B. Goldberg, C.R. Cantor, Proc. Natl. Acad. Sci. USA 103 (2006) 2623.
[6] J.E. Roederer, G.J. Bastiaans, Anal. Chem. 55 (1983) 2333.
[7] R. McKendry, J. Zhang, Y. Arntz, T. Strunz, M. Hegner, H.P. Lang, M.K. Baller, U. Certa, E. Meyer, H.-J. Guentherodt, C. Gerber, Proc. Natl. Acad. Sci. USA 99 (2002) 9783.
[8] Q. Zhang, V. Subramanian, Biosens. Bioelectron. 22 (2007) 3182.
[9] Q. Zhang, L. Jagannathan, V. Subramanian, Biosens. Bioelectron. 25 (2010) 972.
[10] M.E. Roberts, S.C.B. Mannsfeld, N. Queralto, C. Reese, J. Locklin, W. Knoll, Z. Bao, Proc. Natl. Acad. Sci. USA 105 (2008) 12134.
[11] L. Torsi, G.M. Farinola, F. Marinelli, M.C. Tanese, O.H. Omar, L. Valli, F. Babudri, F. Palmisano, P.G. Zambonin, F. Naso, Nat. Mater. 7 (2008) 412.
[12] H.U. Khan, J. Jang, J.-J. Kim, W. Knoll, Biosens. Bioelectron. 26 (2011) 4217.
[13] M. Gollner, M. Huth, B. Nickel, Adv. Mater. 22 (2010) 4350.
[14] H.U. Khan, J. Jang, J.-J. Kim, W. Knoll, J. Am. Chem. Soc. 133 (2011) 2170.
[15] E. Stern, R. Wagner, F.J. Sigworth, R. Breaker, T.M. Fahmy, M.A. Reed, Nano Lett. 7 (2007) 3405.
[16] M.E. Roberts, S.C.B. Mannsfeld, M.L. Tang, Z. Bao, Chem. Mater. 21 (2009) 2292.
[17] H.U. Khan, M.E. Roberts, O. Johnson, R. Förch, W. Knoll, Z. Bao, Adv. Mater. 22 (2010) 4452.
[18] I. Langmuir, J. Am. Chem. Soc. 40 (1918) 1361.
[19] Y. Belosludtsev, I. Belosludtsev, B. Iverson, S. Lemeshko, R. Wiese, M. Hogan, T. Powdrill, Biochem. Biophys. Res. Commun. 282 (2001) 1263.
[20] F.N. Ishikawa, M. Curreli, H.-K. Chang, P.-C. Chen, R. Zhang, R.J. Cote, M.E. Thompson, C. Zhou, ACS Nano 3 (2009) 3969.
[21] F. Liao, C. Chen, V. Subramanian, Sens. Actuators B 107 (2005) 849.
[22] G.H. Gelinck, H.E.A. Huitema, E. van-Veenendaal, E. Cantatore, L. Schrijnemakers, J.B.P.H. van-der-Putten, T.C.T. Geuns, M. Beenhakkers, J.B. Giesbers, B.-H. Huisman, E.J. Meijer, E.M. Benito, F.J. Touwslager, A.W. Marsman, B.J.E. v-Rens, D.M. de-Leeuw, Nat. Mater. 3 (2004) 106.
[23] D.R. Kim, C.H. Lee, X. Zheng, Nano Lett. 9 (2009) 1984.
[24] K.-S. Song, G.-J. Zhang, Y. Nakamura, K. Furukawa, T. Hiraki, J.-H. Yang, T. Funatsu, I. Ohdomari, H. Kawarada, Phys. Rev. E 74 (2006) 041919.
[25] T. Liebermann, W. Knoll, P. Sluka, R. Herrmann, Colloid. Surf. A: Physicochem., Eng. Aspects 169 (2000) 337.